Separation and Purification Technology 306 (2023) 122622

Contents lists available at ScienceDirect

Separation and Purification Technology

journal homepage: www.elsevier.com/locate/seppur

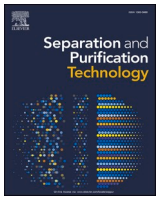

Sustainable recovery of critical elements from seawater saltworks bitterns by integration of high selective sorbents and reactive precipitation and crystallisation: Developing the probe of concept with on-site produced chemicals and energy

V. Vallès [a,b,*], M. Fernández de Labastida [a,b], J. López [a,b], G. Battaglia [c], D. Winter [d], S. Randazzo [c], A. Cipollina [c], J.L. Cortina [a,b,e]

[a] Chemical Engineering Department, Escola d'Enginyeria de Barcelona Est (EEBE), Universitat Politècnica de Catalunya (UPC)-BarcelonaTECH, C/ Eduard Maristany 16, Campus Diagonal-Besòs, 08019 Barcelona, Spain
[b] Barcelona Research Center for Multiscale Science and Engineering, C/ Eduard Maristany 16, Campus Diagonal-Besòs, 08019 Barcelona, Spain
[c] Dipartimento di Ingegneria, Università degli Studi di Palermo, Viale delle Scienze ed. 6, 90128 Palermo, Italy
[d] Fraunhofer Institute for Solar Energy Systems ISE, Heidenhofstraße 2, Freiburg im Breisgau 79110, Germany
[e] CETaqua, Carretera d'Esplugues, 75, 08940 Cornellà de Llobregat, Spain

ARTICLE INFO

Keywords:
Sea mining
Critical raw materials
Saltworks bitterns
Ion exchangers
Circular economy

ABSTRACT

The availability of raw mineral resources containing elements included in the Critical Raw Materials (CRMs) list is a growing concern for the European Union. Sea mining has been identified as a promising secondary source. In particular, brines obtained in solar saltworks (bitterns) contain relevant amounts of valuable CRMs such as Mg (II), B(III), other alkaline/alkaline earth metals (Rb(I), Cs(I), Sr(II)) and transition/post-transition elements (Co (II), Ga(III), Ge(IV)). However, the low concentration of some of these elements (μg/L) requires an effort to develop recovery routes that are sustainable and economically feasible where the required chemicals and energy are produced on-site from the saltworks bitterns (i.e. HCl and NaOH). Even the conventional recovery processes such as ion exchange, sorption and precipitation, which have proved to be competitive for metals recovery, are challenged in the case of Trace Elements (TEs). This work studies the recovery of TEs included in the CRMs list from saltworks bitterns after ion exchange processes. First, batch crystallisation and reactive precipitation were tested for some target elements in single-component solutions: Sr(II), Co(II), Ga(III), Ge(IV) and B(III). Then, the experiments were carried out with multi-component synthetic solutions assuming different scenarios of bittern streams coming out a selective extraction stage using sorption and ion exchange processes. The targeted elements were recovered except for Ge(IV), where alternative routes need to be evaluated, as its precipitation involves the use of tannic acid or sulphide solutions that could not be produced from the bitterns. However, a further concentration step would be necessary to achieve element concentrations closer to the mineral phases saturation. Moreover, model simulations were performed using the PHREEQC program, which provided a good prediction of the experimental trends obtained in most cases.

1. Introduction

Securing the availability and sustainable supply of Critical Raw Materials (CRMs) is crucial for technological progress and the global economy [1]. Therefore, reliable and unhindered access to certain raw materials is a growing concern that motivates finding new secondary sources to overcome the current limitations from typical sources such as mines and ores [2].

Sea mining has been identified as a promising option since it contains almost all the periodic table elements [3–7]. Direct use of seawater has been extensively studied in the literature for the recovery of crucial elements such as Mg(II), Li(I), Rb(I) or Sr (II). However, some CRMs are

* Corresponding author at: Chemical Engineering Department, Escola d'Enginyeria de Barcelona Est (EEBE), Universitat Politècnica de Catalunya (UPC)-BarcelonaTECH, C/ Eduard Maristany 16, Campus Diagonal-Besòs, 08019 Barcelona, Spain.
E-mail address: victor.valles.nebot@upc.edu (V. Vallès).

https://doi.org/10.1016/j.seppur.2022.122622
Received 1 September 2022; Received in revised form 7 November 2022; Accepted 8 November 2022
Available online 13 November 2022

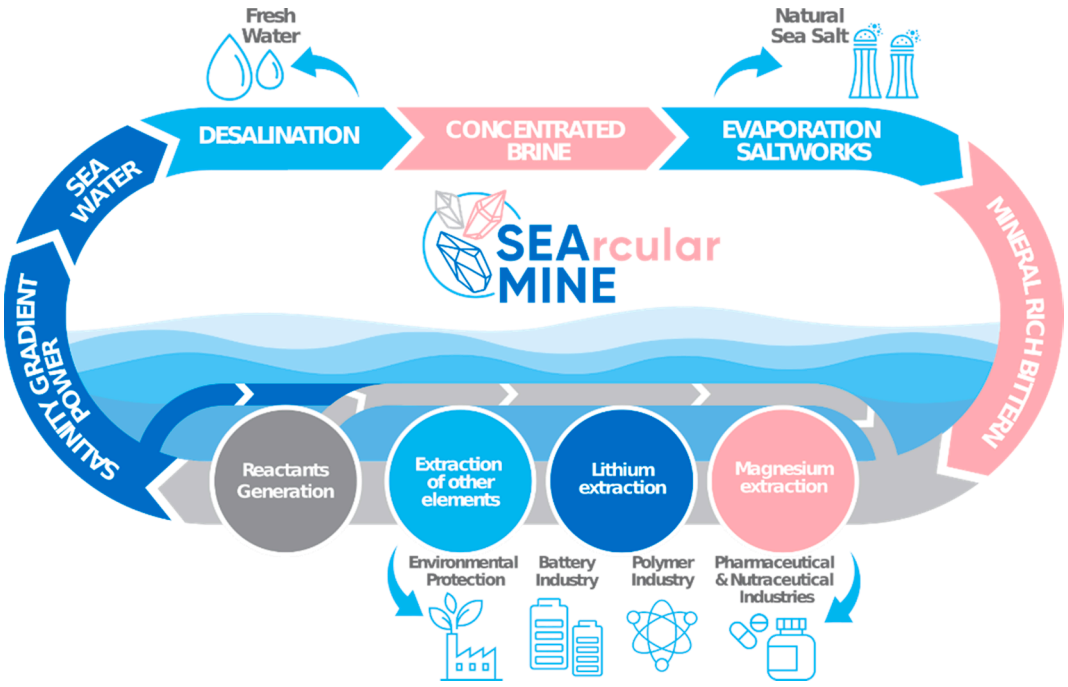

Fig. 1. Simplified scheme of the SEArcularMINE concept [32].

present at low concentrations (mg/L and μg/L), complicating their recovery. A different approach consists of recovering in-land seawater brines as reverse osmosis desalination and saltworks bitterns. Seawater desalination produces highly concentrated brines where the concentration of the elements is significantly higher than in seawater (considering a water recovery of 50 %, they are double concentrated than in seawater) [8]. Nonetheless, lower element recovery from brine could reduce potable water costs and the environmental impact of desalination plants caused by brine disposals.

In the case of saltworks, seawater flows through a system of shallow ponds where the natural process of evaporation and fractionated crystallisation occurs, producing sea salt and brine, so-called bittern, free of Ca(II) as a by-product. Bitterns generated in saltworks are 20–40 times more concentrated than seawater in some elements included in the CRMs list, such as Mg(II) (up to 70 g/L) and other alkaline/alkaline earth metals (e.g. Li(I), Sr(II)) and transition/post-transition elements (e.g. Co(II), Ga(III), Ge(IV)).

Although those brines are highly concentrated compared to seawater, the economic viability of extracting Trace Elements (TEs) (those at μg/L) is still challenging due to the low concentration, the limited selectivity and brine solutions complexity. Therefore, it is necessary to develop recovery routes that fulfil economic and sustainability criteria.

In this context, the European project SEArcularMINE (https://www.searcularmine.eu) focuses on developing novel technologies to recover valuable minerals from seawater bitterns of the Mediterranean area. The project targets CRMs such as Mg(II), Li(I), B(III) and TEs belonging to the alkaline/alkaline earth metals (e.g. Rb(I), Cs(I), Sr(II)) and transition/post-transition metals (e.g. Co(II), Ga(III), Ge(IV)) groups. However, one of the most relevant proposals of the project is the on-site production of the chemicals requested to recover the target elements in the form of marketable minerals using the main components of the saltworks bitterns (NaCl, Na_2SO_4, KCl). The proposed treatment scheme introduces the use of separation processes where NaOH, KOH, HCl and H_2SO_4 will be produced by integration of electrodialysis with bipolar membranes as it has been previously postulated [9–11].

In relation to the TEs of interest of the project, Rb(I) and Cs(I) are valuable and useful for a wide range of applications [12]. They are found as complex minerals, so the mining difficulty makes them scarce. Therefore, it is essential to recover both of them from alternative sources to reduce the dependence on primary mineral ones. Thus, in the literature it can be found studies about extraction of Rb(I) and Cs(I) using ion exchange [12,13], solvent extraction [14], reverse osmosis [15] or membrane distillation [16]. Sr(II) is the least abundant of all alkaline earth metal elements. It can be obtained by leaching its most commonly mineral forms, such as celestite ($SrSO_4$(s)) and strontianite ($SrCO_3$(s)), or from brines and other liquid wastes. Among the different techniques studied to extract Sr(II), adsorption has been identified as a promising one [17,18], although there are limited studies applied to the case of seawater [19]. As for the transition and post-transition elements, Co(II) is mainly extracted from ores and other compounds ores. Moreover, several technologies have been developed to recover Co(II) from wastewater or natural aqueous solutions such as chemical precipitation, adsorption, membrane or ion exchange [20]. Ga(III) is mainly produced as a by-product of bauxite refining to produce alumina (Bayer process) and from zinc residues treatment [21]. However, regarding the low content in primary resources, acid/alkaline leaching hydrometallurgical processes have also been studied in the literature [22,23]. Ge(IV) is mined from sulphide ores of zinc, lead and copper, coal deposits and is also obtained as a by-product of these ores and coals. Then, the main established technologies for Ge(IV) recovery are based on hydrometallurgical processes complemented with concentration techniques such as solvent extraction, absorption and ion exchange [24,25]. Finally, B(III) is also present in seawater and brines at such a concentration level (4–5 mg/L in seawater), making its recovery attractive since it is also an element widely used in the industry. In the literature, numerous studies are devoted to B(III) recovery through chemical precipitation, adsorption, reverse osmosis, electrodialysis, solvent extraction, and ion exchange [26–30].

Within the SEArcularMINE project scope, the bittern resulting from saltworks is treated via ion exchange to selectively extract TEs that are recovered subsequently in dedicated crystallisation units. The selective or quasi-selective separation of the target groups of elements has been previously developed in a separate study [31]. Fig. 1 represents a simplified scheme of the SEArcularMINE concept describing: i) the recovery of the different targeted minerals from the saltworks brines

Table 1
Solubility values for the TEs investigated in different mineral phases, calculated considering a water density of 1000 g/L [33–38]. (n.a.: not available)

Target element	Mineral phase	Solubility g/100 g H_2O	log K_{so}
Sr	$SrCO_3$(s)	0.00034	9.3
	$SrSO_4$(s)	0.0135	6.6
	$Sr(OH)_2$(s)	2.25	−28.5
Rb	Rb_2CO_3(s)	223	−8.3
	Rb_2SO_4(s)	58.8	1.0
	RbOH(s)	173	−25.8
	RbCl(s)	93.9	1.3
B	H_3BO_3(s)	2.62	0.07/0.16
	B_2O_3(s)	2.77	−5.6
	$Na_2B_4O_7$(s)	2.58	−21.4
	$Na_2B_4O_7{\cdot}7H_2O$(s)	n.a.	−17
Cs	Cs_2CO_3(s)	260.5	−11.3
	Cs_2SO_4(s)	167	0.9
	CsOH(s)	395	−27.5
	CsCl(s)	186	1.3
Co	$CoCO_3$(s)	0.00014	9.98
	$CoSO_4$(s)	33	17.5
	$Co(OH)_2$(s)	0.00032	−12.2
	$CoCl_2$(s)	53	11.8
Ga	GaOOH(s)	n.a.	−2.9/−1.5
	$Ga(OH)_3$(s)	n.a.	−11.9
	$GaCl_3$(s)	n.a.	−18.0
	$Ga_2(SO_4)_3$(s)	n.a.	n.a.
Ge	GeO_2(s)	0.447	4.96
	$Ge(SO_4)_2$(s)	n.a.	n.a
	$Ge(CO_3)_2$(s)	n.a.	n.a
	$GeCl_4$(s)	n.a.	n.a

where, additionally to TEs, Mg(II) and Li(I) are also postulated to be recovered and ii) the production of auxiliary chemicals (e.g. NaOH, KOH, HCl, H_2SO_4 and Na_2SO_4) using electrodialysis with bipolar membranes to integrate the full recovery scheme.

This paper studies the use of evaporation/crystallisation for B(III) recovery and reactive precipitation processes for TEs (Sr(II), Co(II), Ge (III) and Ga(IV)). A critical review of the geochemical databases was used to identify which minerals phases could be produced by using those chemicals that could be on-site produced from the main components of the saltworks bitterns (i.e. HCl and NaOH). Two sets of experimental tests were carried out evaluating the recovery: i) from single TEs components mimicking the case of incorporating a selective sorbent extracting the target ion, and ii) from solutions mimicking the expected streams coming out the ion exchange extraction stage from bitterns where the sorbents used are not providing enough selectivity. Those single- and multi-component solutions generated after the desorption stage of the TEs sorbents will contain HCl, as the sorbents selected are regenerated using 1 M HCl. As the recovery of TEs by sorption/ion exchange processes could be performed in different stages, the composition of the expected streams generated is different and the study considered four different scenarios. The study will identify the optimum chemical conditions (e.g. concentration, pH conditions, evaporation ratios) where the maximum recovery ratios are achieved and what are the mineral phases of the minerals recovered.

2. Materials and methods

2.1. Chemicals

The following chemicals were used: NaCl (>99.9 %, Glentham LIFE SCIENCES), KCl (>99 %, Sigma-Aldrich), $MgCl_2{\cdot}6H_2O$ (>99 %, Sigma-Aldrich), $CaCl_2{\cdot}6H_2O$ (98 %, Sigma-Aldrich), LiCl (>99 %, Sigma-Aldrich), H_3BO_3 (>99.5 %, Sigma-Aldrich), $CoCl_2{\cdot}6H_2O$ (>98 %, Alfa Aesar), Rb_2CO_3 (99 %, Sigma-Aldrich), $SrCl_2{\cdot}6H_2O$ (>98 %, Alfa Aesar), CsCl (>99.9 %, Glentham LIFE SCIENCES), Na_2SO_4 (>99.5 %, Glentham LIFE SCIENCES), NaBr (>99 %, Sigma-Aldrich), HCl (37 %, Sigma-Aldrich), NaOH (>97 %, Glentham LIFE SCIENCES), Ge ICP Standard (10000 mg/L, Alfa Aesar) and Ga ICP Standard (10000 mg/L, Alfa Aesar).

Table 2
Composition (mg/L) of multi-component solutions used in the TEs crystallisation experiments for each scenario.

Scenario	1	2	3	4
Na(I)	5162	15377	15932	5913
Mg(II)	7349	4	619	578
Ca(II)	225	77	31	1026
K(I)	920	1530	1803	572
S(VI)	8438	9950	12457	3345
B(III)	1722	1560	28	28
Li(I)	70	0.07	0.06	0.11
Sr(II)	0.40	15	12	152
Co(II)	0.90	2	65	141
Ga(III)	0.40	0.50	47	0.07
Ge(IV)	0.14	13	0.10	0.20

2.2. Preparation of trace elements containing solutions for evaporation/crystallisation and reactive precipitation experiments

A preliminary solubility analysis of TEs in their different mineral phases, using chemical and geochemical databases [33–38], was performed to delineate the most favourable precipitation condition, as reported in Table 1.

As discussed in the introduction, TEs are characterised by very low concentrations in the bitterns (μg/L levels). In this case, the precipitation process represents a promising option. To precipitate any compound, its solubility limit must be lower than its concentration in the solution. Therefore, TEs sparingly soluble compound were chosen among their mineral phases. Specifically, from Table 1, it can be seen that: i) Sr(II) can be precipitated both as carbonate or as sulphate; ii) Rb(I), B(III) and Cs(I) present high solubility values for each of their mineral phases, therefore they cannot be easily recovered by precipitation, unless an evaporation stage is performed; iii) Ga(III) could be precipitated as hydroxide, and iv) Ge(IV) could be recovered as oxide.

TEs crystallisation experiments were performed in the case of i) single-component solutions considering the availability of highly selective sorbents able to produce an eluate with TEs concentrations up to 200 mg/L (in 0.1 M HCl) and ii) multi-component solutions, considering partially selective ion exchange/sorbents. In the second case, the aim was to mimic the expected compositions coming out ion exchange elution stage under four different scenarios in 1.0 M HCl:

- Scenario 1: Recovery of B(III) from an eluate after treating a high salinity bittern with a selective ion exchange resin for B(III);
- Scenario 2: Recovery of B(III) from an eluate after treating a high salinity polished (low contents of Mg(II) and Ca(II)) bittern with a selective ion exchange resin for B(III);
- Scenario 3: Recovery of Ga(III) and Co(II) from an eluate after treating, with a selective ion exchange resin for Ga(III) and Co(II), the bittern expected at the TEs-recovery unit;
- Scenario 4: Recovery of Sr(II) from an eluate after treating, with a selective ion exchange resin for Sr(II), the bittern expected at the TEs-recovery unit.

These scenarios were postulated under the results developed in a large screening study, where 30 ion exchange resins were evaluated with the different streams to be generated in the SEArcularMINE recovery concept, as it was described in a previous study of some co-authors [31].

2.2.1. Trace elements single-component solutions

The concentration was set to 200 mg/L in a 0.1 M HCl matrix solution except in the case of B(III) where the concentration was 2500 mg/L.

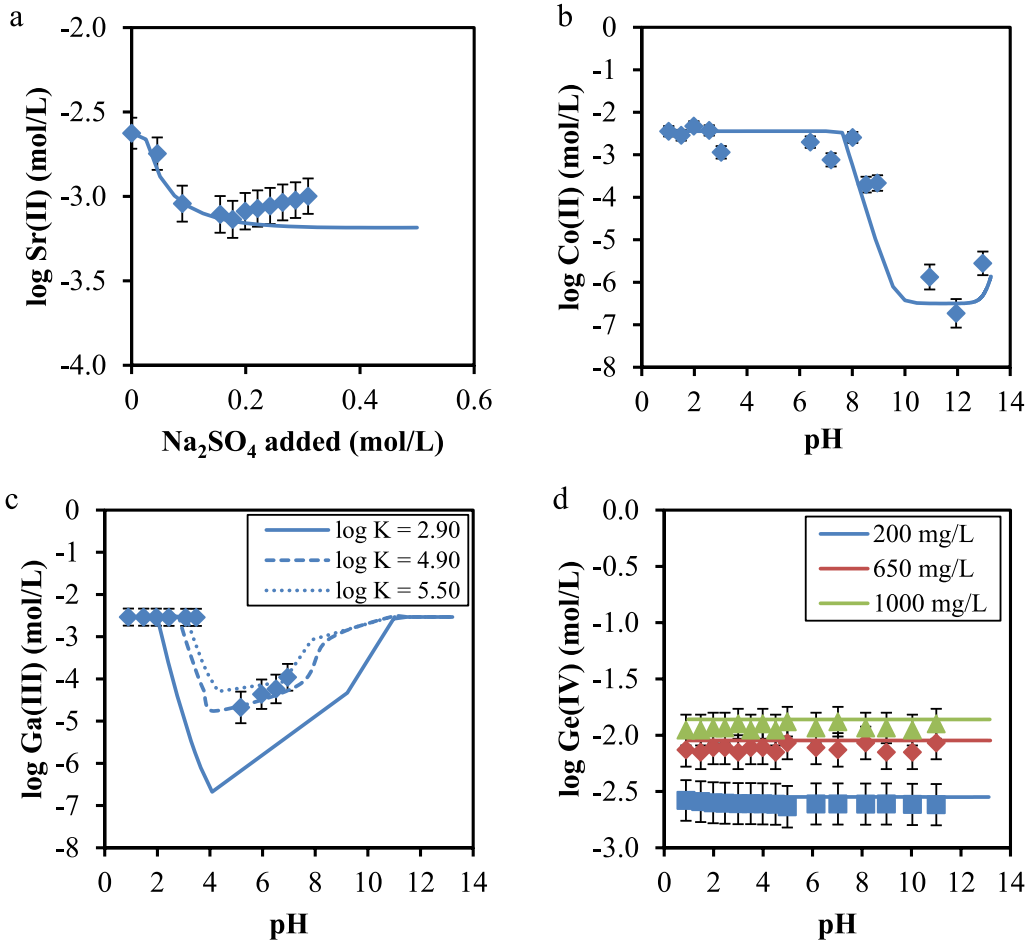

Fig. 2. Logarithm of molar concentration (log_{10}) of (a) Sr(II) as a function of Na_2SO_4(s) added; (b) Co(II), (c) Ga(III) and (d) Ge(IV) as a function of pH. Points: experimental data, lines: PHREEQC simulation considering the formation of celestite ($SrSO_4$(s)) for the case of Sr(II), $Co(OH)_2$(s) for Co, GaOOH(s) and two other for soluble phases of $Ga(OH)_3$(s) ($logK_{so}$ = 4.9 and $logK_{so}$ = 5.5 respectively) for Ga(III) and GeO_2(s) for Ge (IV).

Additionally, two concentrations more were also studied for Ge(IV), 650 mg/L and 1000 mg/L. The concentration level of 200 mg/L was selected as it was estimated that this level would be achieved in the regeneration of the ion exchange resins after using them to treat the bittern (values reported by Vicari et al. [39]). Na_2SO_4(s) was used as a precipitant for Sr (II), while for the rest of elements it was used 1 M NaOH. In the case of B (III), an evaporative route was used to crystallise boric acid (H_3BO_3(s)).

2.2.2. Trace elements multi-component solutions

Table 2 shows the composition of the four multi-component solution scenarios used for the crystallisation experiments carried out. These compositions were the real ones obtained in the regeneration of the ion exchange resins after using them to treat bitterns with the expected composition of TEs. The matrix solution was 1.0 M HCl.

2.3. Routes for recovery of trace elements following a reactive precipitation and evaporation/crystallisation stages

2.3.1. Reactive precipitation

The precipitation experiments were carried out with an initial volume of 800 mL. Solutions used were those described as scenarios 3 and 4 (see Table 2) and the single-component solutions (except for B(III)). The solution was continuously stirred, and the pH was monitored throughout the experiments using a pH-meter (GLP 22, Crison) measuring in-line. The solution pH was gradually increased by adding 1 M NaOH, and liquid samples were taken during the experiments to monitor the composition changes of the solution. The generated bulk precipitate was recovered by filtration using a 0.22 μm pore size filter. The experiments were stopped once a value of pH 12 was reached. For Sr (II) recovery, Na_2SO_4(s) was added in order to saturate the solution and favour the precipitation of celestite ($SrSO_4$(s)). In the case of the single-component experiment, no NaOH was added.

In some cases, staged precipitation was performed to obtain a series of precipitates in different pH ranges. In this way, the pH was increased up to a target value and the solid was recovered by filtration. After that, the filtrate was subjected to further pH increase, followed by another filtration step.

2.3.2. Evaporation

The evaporation experiments were performed only for B(III) recovery. In this case, the initial volume was 500 mL and a hot plate magnetic stirrer (C-MAG HS 7, IKA) was used to keep the solution continuously stirred at 70 °C. A sample was taken every 50 mL to monitor the composition changes during the experiment. The measurements were stopped after 400 mL were evaporated. The final solution was cooled down to room temperature to favour the precipitation of salts. After that, the solution was filtrated using a 0.22 μm pore size filter.

2.4. Prediction of the expected concentrations along the reactive precipitation and crystallisation by using PHREEQC as equilibrium tool

The variation of concentrations along the crystallisation experiments was simulated with the PHREEQC (version 3.6.2) numerical code [40]. Due to the high-salinity of the solutions, the Pitzer database was used.

However, it only includes the major elements (e.g. alkalinity, Na(I), K(I), Ca(II), Mg(II), S(VI) and Cl(-I)), whereas there is no data regarding the TEs. Therefore, the Pitzer database was extended with values extracted from the literature in order to include them as reported by Vicari et al. [39]. Furthermore, withdrawing of mineral phases that precipitate along the process was imposed.

2.5. Analytical techniques

The composition of liquid samples was determined by Inductively Coupled Plasma Mass Spectrometer (7800 ICP-MS) and Optical Emission Spectrometer (5100 ICP-OES) from Agilent Technologies. pH was monitored throughout the experiments by using a pH-glass electrode (GLP 22, Crison).

Solid samples were dried in an oven at 40 °C for 48 h. Its morphology was obtained by Field Emission Scanning Electron Microscopy Energy Dispersive X-ray Spectroscopy (FESEM-EDS) (JEOL JSM-7001F) at an acceleration voltage of 20.0 keV Secondary Electron Imaging (SEI) or Backscattered Electrons (BE).

The mineral phases were identified with X-ray Diffraction (XRD) after grinding the sample into powder. A D8 Advance diffractometer (Bruker) was used with a Bragg-Brentano configuration θ-2θ and a vertical goniometer. The equipment has a Cu X-ray tube, which allows to work up to 40 kV and 40 mA. The spectrum was recorded from 15° to 60° with steps of 0.020°. The identification of mineral phases was performed with EVA software (Bruker).

3. Results and discussion

3.1. Recovery of trace elements from single-component solutions reproducing extraction schemes with highly selective sorbents

Fig. 2 shows the logarithm of molar concentration of the different elements (Sr(II), Co(II), Ga(III) and Ge(IV)) as a function of the total Na_2SO_4 concentration added or as a function of pH. Points represent the experimental data and lines the PHREEQC prediction. The fraction diagrams of Sr(II), Co(II), Ga(III) and B(III) in each solution are shown in (Figs. S1-S4) in Supplementary Information. Ge(IV) fraction diagram is provided within the text of the manuscript.

For Sr(II) (Fig. 2.a), Na_2SO_4(s) was added in solid form to achieve saturation of celestite ($SrSO_4$(s)). It can be observed that Sr(II) concentration decreased as sulphate ions were added into the solution, which allowed recovering the 68 % of the initial content. PHREEQC simulations were carried out with the Pitzer package developed by Vicari et al. [39], and it can be observed that the database fitted properly the experimental data. However, at the highest Na_2SO_4(s) dosages (>0.2 mol/L) several deviations between the model and experimental data were observed.

Regarding Co(II) (Fig. 2.b), it can be observed that Co(II) started to precipitate approximately at pH 8, and it completely precipitated at pH 11–12 (>99.99 %). PHREEQC with the Pitzer modified database predicted properly the precipitation of Co(II) as $Co(OH)_2$(s), predicting also the re-dissolution of Co observed at pH >12.

In relation to Ga(III) (Fig. 2.c) it started to precipitate at pH 4, and it was completely recovered at pH 5–7. However, at higher pH values, Ga (III) re-dissolved into the solution. PHREEQC model anticipated the precipitation of Ga(III) as GaOOH(s) at pH 2, reaching its lowest concentration at pH 2.7 (2 mg/L) and then started to re-dissolve into the solution. At pH higher than 11, GaOOH(s) is expected to be completely dissolved. However, as the FESEM-EDS analysis shown in Fig. S5.c, Ga (III) precipitated mineral phases, rich in O and Ga, had a flatten-shape, but no peaks were observed with the XRD analysis (data not shown) indicating an amorphous nature. Ga(III) chemistry is having a similar chemistry behaviour as Fe(III) and Al(III) forming FeOOH(s) and AlOOH (s) minerals phases with $\log K_{so}$ of −1.0 and −8.5 respectively while GaOOH(s) is having a log K_{so} of −2.9 [40]. However, when Al(III) and Fe

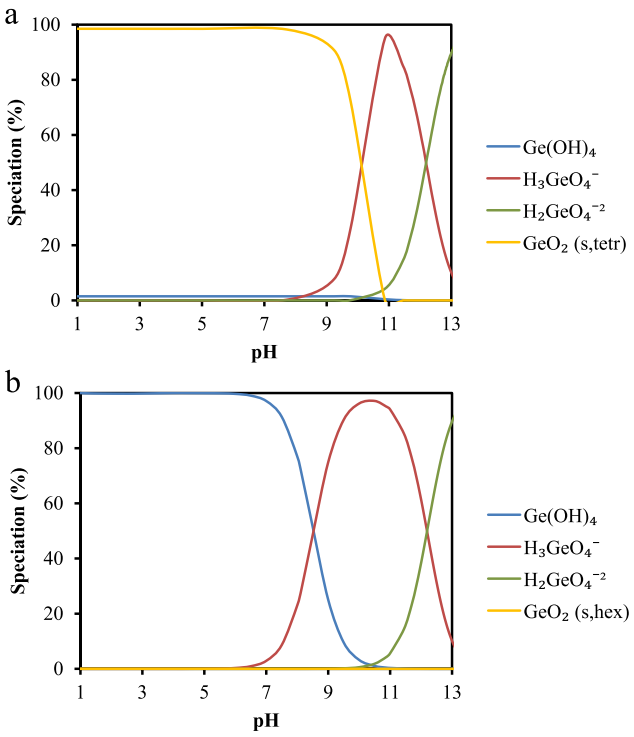

Fig. 3. Fraction diagram for Ge(IV) single-component solution as a function of pH considering Ge(IV) precipitation as GeO_2(s) in (a) tetragonal structure and (b) hexagonal structure. Data was obtained by PHREEQC simulations.

(III) are precipitated in acidic hydrochloric solutions tend to form amorphous mineral phases as $Fe(OH)_3$(s) and $Al(OH)_3$(s) of higher solubility with up to two and four order of magnitude of higher solubility constants (-5.0 and −10.4 respectively). Assuming a similar behaviour for Ga(III) and, considering that solubility constants were not available in literature, their increase between 2 and 2.5 order of magnitude, the predicted values by PHREEQC (dotted lines in Fig. 2.c) provide a better description of the measured values.

Fig. 2.d shows the logarithm of the Ge(IV) molar concentration as a function of pH. Initially, experiments were performed with 200 mg/L. However, no precipitates were observed. Therefore, two additional experiments at higher concentrations (650 and 1000 mg/L) were conducted, but the Ge(IV) concentrations did not vary in the entire pH range and, therefore, GeO_2(s) did not precipitate. Simulations performed with PHREEQC stated that the element that should precipitate was the GeO_2(s) with a tetragonal shape (see Fig. 3.a), which did not take place neither at the pH range or the concentrations evaluated. Instead, by forcing that the mineral phases that should precipitate has to have a hexagonal structure (Fig. 3.b), the model was able to fit properly the

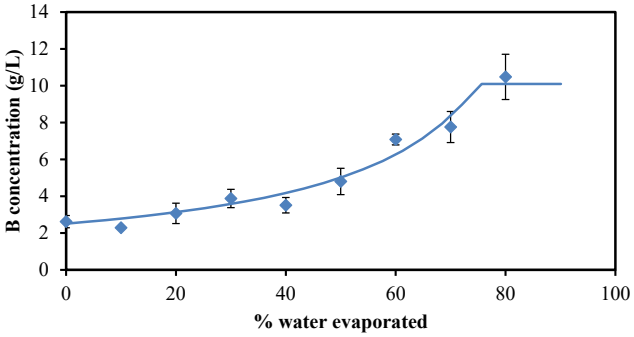

Fig. 4. Concentration of B(III) as a function of % water evaporated. Points: experimental data, lines: PHREEQC simulation.

Table 3
Maximum recovery factor (%) for the target TEs from the single-component solutions, the reagent and energy (thermal/electrical) for mineral phase formation and the mineral composition of the recovered by-products. Initial concentration of the target TEs and the conditions under which the solids were obtained are provided.

Element	Initial concentration (mg/L)	Route for recovery	Reagent or energy	Mineral composition	Recovery (%)	Conditions
Sr(II)	207	Reactive precipitation	Na_2SO_4(s)	$SrSO_4$(s)	68 %	0.18 mol/L of Na_2SO_4
Co(II)	211	Reactive precipitation	1.0 M NaOH	$Co(OH)_2$(s)	>99 %	8 < pH < 12
Ga(III)	204	Reactive precipitation	1.0 M NaOH	GaOOH(s)	>99 %	5 < pH < 7
Ge(IV)[a]	191 537 805	Reactive precipitation	1.0 M NaOH	No precipitation observed	–	–
Ge(IV)[b]	90	Reactive precipitation	Tannic acid	Tannin complex[c]	>99 %	125 mg tannic acid per 100 mL of solution (pH < 0)
Ge(IV)[d]	35–1623 (in 6.0 N HCl media)	Reactive precipitation	H_2S(g)	GeS_2(s)	>99 %	100 % H_2S(g) or 50:50 H_2S/CO_2 gas mixture flushing
B(III)	2620	Evaporation	Heat electrical energy	H_3BO_3(s)	51 %	80 % water evaporated

[a] Results from this study.
[b] Results from Arroyo-Torralvo et al. [42].
[c] $H_2(GeO_2C_{76}H_{52}O_{46}{\cdot}nH_2O)$(s) [44].
[d] Results from Arroyo et al. [45].

data. According to the literature, the most effective way to recover Ge (IV) is by using tannic acid. Tannic acid ($C_{76}H_{52}O_{46}$), or decagalloyl glucose, is a mixture of polygalloyl glucoses or polygalloyl quinic acid esters with the number of galloyl moieties per molecule ranging from 2 up to 12 depending on the plant source used to extract the tannic acid [41–43]. For instance, Drzazga [41] precipitated Ge(IV), for an initial concentration of 6 g/L, using tannic acid at temperatures higher than 60 °C. In a similar study, Arroyo-Torralvo [42] achieved the recovery of Ge(IV) (>99 %) from a solution containing 90 mg/L Ge(IV) by using tannic acid.

Experiments for B(III) recovery were performed by evaporating water until reaching H_3BO_3(s) saturation (Fig. 4). Starting from a B(III) concentration of 2.62 g/L, it increased until reaching values of 10.5 g/L after evaporating 80 % of the water. In these conditions, boric acid (H_3BO_3(s)) started to precipitate once the solution was cooled down. PHREEQC totally predicted the behaviour of B(III). The fraction diagram for the B(III) solution is displayed in Fig. S4.

Fig. S5 shows the FESEM images of the precipitates collected, from these single-component solutionts performances, at 2.00 keV. XRD results are also collected in Supplementary information (Figs. S6–S8). It can be observed that Sr(II) crystals (Fig. S5.a) have a regular and elongated shape and XRD analysis confirmed that the mineral phase that precipitated was celestite ($SrSO_4$(s)). Narrow and high peaks from the XRD show that the structure obtained is a solid of high purity. The precipitates of Co(II) (Fig. S5.b), which were β-$Co(OH)_2$(s) according to XRD, have an irregular shape and a low crystallinity (low-intensity peaks). Ga(III) precipitates were just a powder that, after being filtered, formed a thin layer (Fig. S5.c). In this case, no peaks were observed in XRD analysis (data not shown). In relation to the characterisation of the B(III) crystals collected (Fig. S5.d), it can be observed that they present an irregular shape and, according to XRD, they were sassolite (H_3BO_3(s)).

From the experiments performed from solutions mimicking a separation scheme where the selectivity of the sorbents is providing high selective separation, the highest recovery factors (%) that could be achieved are summarised in Table 3. In addition, two other strategies are reported regarding Ge(IV) precipitation. The recovery factor was calculated as indicated in equation (1).

$$\text{Recovery}(\%) = 100{\cdot}(1 - m/m_0) \quad (1)$$

Where m is the mass of target element that remains in solution and m_0 is the mass of target element in solution at the beginning of the precipitation process.

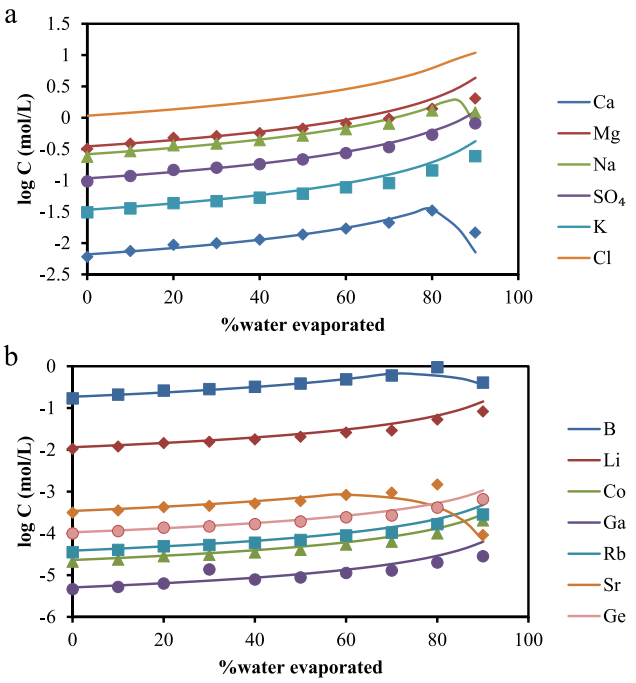

Fig. 5. Logarithm (log_{10}) of molar concentration of (a) major and (b) minor components as a function of %water evaporated for the brine rich in B(III) and Mg(II) (scenario 1). Points: experimental data, lines: PHREEQC simulation.

In the case of the elements as Co(II), the recovery could be also achieved with Na_2CO_3(s) by using a mixture of NaOH(s) with CO_2(g) that would be accessible chemical due to the efforts on CO_2(g) sequestration in the next years. In the case of B(III), that is requiring large evaporation ratios to be recovered as H_3BO_3(s), the precipitation of Ca borates ($Ca(B_3O_4(OH)_3){\cdot}H_2O$(s)) by using mixtures of $CaCl_2$ and NaOH, also potentially recovered from saltworks bitterns, could be an alternative to be used. Finally, in the case of Ge(IV), three case are reported in the Table 3, highlighting that it seems that the use of tannic acid or H_2S (g) is required to recover GeO_2(s) or GeS_2(s), respectively, from the regenerated streams, as done by Arroyo et al. [42,45].

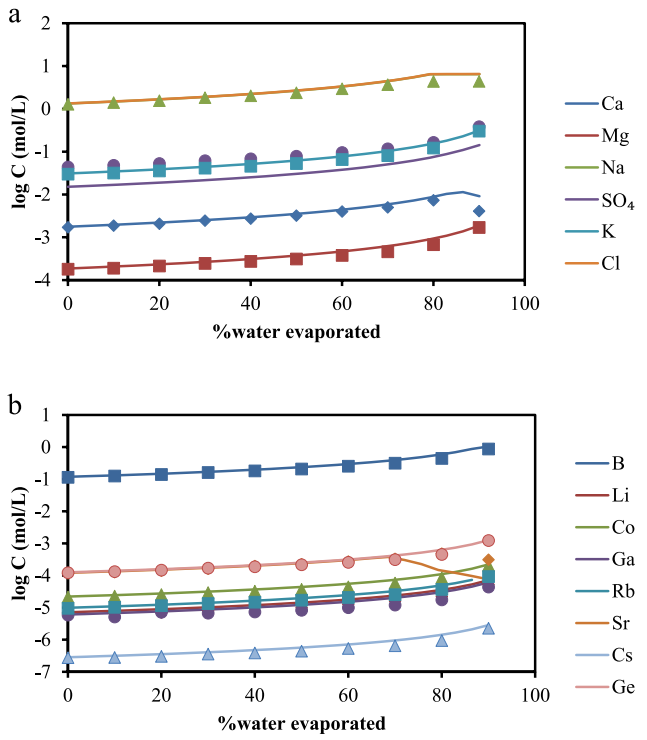

Fig. 6. Logarithm (log_{10}) of molar concentration of (a) major and (b) minor components as a function of % water evaporated for the brine rich in B(III) after Mg(II) and Ca(II) polishing (scenario 2). Points: experimental data, lines: PHREEQC simulation.

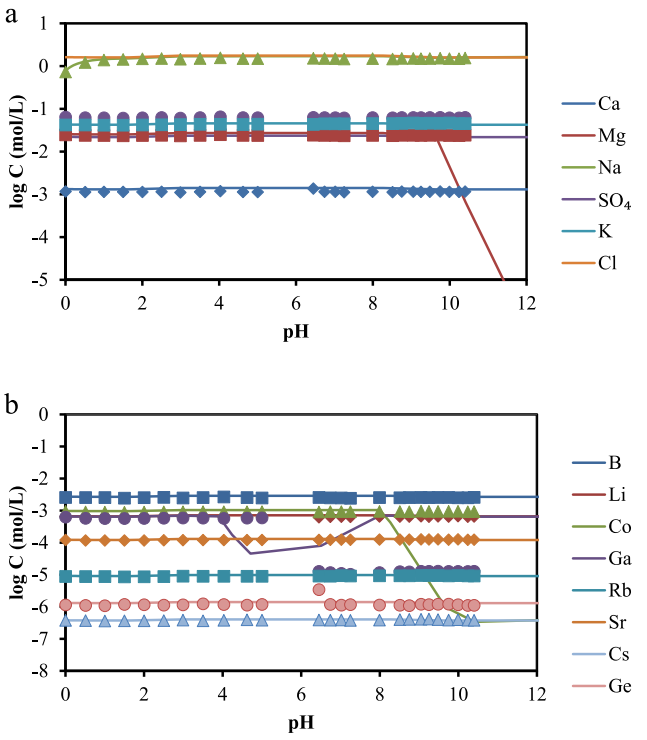

Fig. 7. Logarithm (log_{10}) of molar concentration of (a) major and (b) minor components as a function of pH for the Ga(III) and Co(II) recovery for the expected brine (scenario 3). Points: experimental data, lines: PHREEQC simulation.

3.2. Recovery of trace elements from multi-component solutions reproducing extraction schemes with partially selective sorbents

3.2.1. Boron recovery

Evaporation was tested as a recovery route for B(III) from the brine rich in B(III) and Mg(II) (scenario 1, Table 2). Fig. 5.a and Fig. 5.b show the variation of the concentration as a function of the percentage of water evaporated for major and minor components, respectively. Two main behaviours could be expected, depending on the solubility of the mineral phases: i) the ions not forming any mineral phase during the evaporation should increase their concentration as a function of the evaporation ratio, while ii) those forming a mineral phase would decrease their concentration due to precipitation. B(III) concentration increased from 1.84 g/L to 10.25 g/L when the 80 ± 5 % of the water was evaporated, and it started the precipitation of boric acid (76 % recovery). It can be seen how the precipitation also occurred for Na(I), Ca (II) and Sr(II) once 80 ± 5 % of evaporation was reached. PHREEQC was able to fit all the experimental results, predicting quite well the precipitation of H_3BO_3(s), NaCl(s) and Sr(II) as $SrSO_4$(s), although the precipitation of Sr(II) and H_3BO_3(s) are predicted to start once 60 % and 70 % of water is evaporated, respectively, instead of the 80 % observed experimentally.

FESEM images and EDS spectra of the collected solids reported in Fig. S9 allowed determining the composition of the precipitated solids. B (III) content ranged between 20 and 30 %, identifying the precipitation of boric acid. Moreover, NaCl(s) and $Mg(OH)_2$(s) were also present at relatively lower amounts (<2 %), but no traces of Sr(II) were found. In this case, XRD analysis indicated the presence of sassolite (H_3BO_3(s)), in addition to halite (NaCl(s)) (see Supplementary information, Fig. S10), as predicted by PHREEQC (see Supplementary information, Fig. S11).

For the case of the brine rich in B(III) after Mg(II) and Ca(II) polishing (scenario 2), the results are shown in Fig. 6. The initial B(III) concentration was 1.24 g/L and it increased up to 9.42 g/L during the evaporation. As shown in Fig. 6.a, only the Na(I) and Ca(II) precipitated. Although PHREEQC predicted Sr(II) precipitation to a lesser extent (Fig. 6.b), it was not observed.

From Fig. S12, where are reported FESEM images and semi-quantitative analysis given by the EDS spectra of the collected solid, it is evident that the recovered solids after evaporation are made of NaCl, as observed in the previous case. In fact, XRD spectra revealed only the presence of halite (NaCl). In order to avoid halite crystallisation, another route focused on B reactive precipitation could be followed. Yilmaz et al. [46], for example, successfully recovered B as $CaB_3O_3(OH)_5{\cdot}4H_2O$(s) from wastewater under different conditions adding $Ca(OH)_2$(s). Considering a conditions set similar to the ones in the current study, they were able to precipitate around 97 % B in a 120 min reaction at a pH 1 and 80 °C after adding 10 g of $Ca(OH)_2$(s) to 500 mL of an initial solution containing 1000 mg/L B.

3.2.2. Trace elements (Co, Ga, Sr) recovery by reactive precipitation

Fig. 7 shows the results obtained during the precipitation for the Ga (III) and Co(II) recovery from the expected brine (scenario 3). NaOH was added from pH 0 to 10, and solids were collected at pH 5 and 10 to recover selectively Ga(III) and Co(II).

Interestingly, experimental results show that Ga(III) precipitates at pH 5 (Fig. 7.b), remaining with a concentration two orders of magnitude lower after filtration (recovery of >99 %). It can be observed that by a further increase of the pH, the other elements potentially forming hydroxides (e.g. Cs(I), Rb(I), Sr(II), Ge(IV)) did not precipitate. When comparing the predictions derived by PHREEQC, Ga(III) precipitation was expected to start at pH 4, assuming a removal of 93 % at pH 4.8.

By further increasing the pH to 10, regarding Co(II), which was expected to be recovered as $Co(OH)_2$(s), it did not precipitate despite the PHREEQC estimated its removal at pH 8, indicating that higher preconcentration factors should be achieved to precipitate it. Additionally, it was expected that $Mg(OH)_2$(s) started to precipitate at pH 9.8 taking into account the Mg(II) amount present in the brines. The model solution had a content of Co(II) below 0.1 g/L and maybe more insoluble

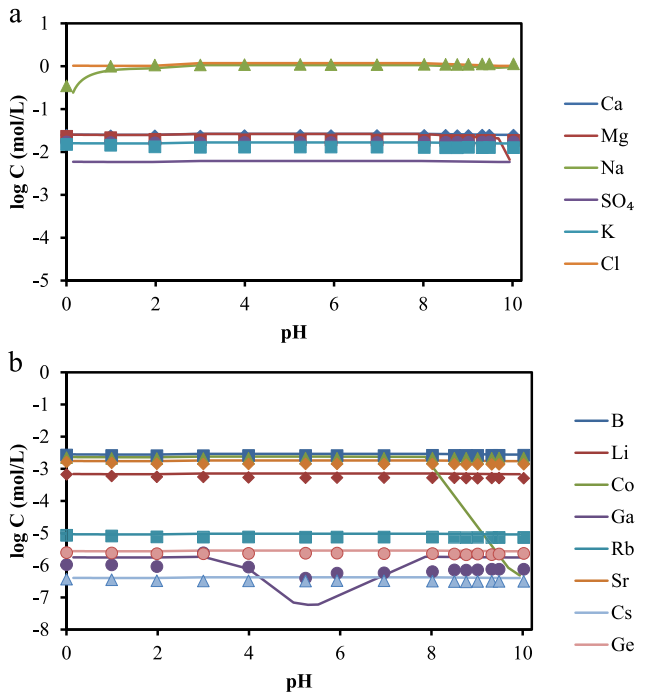

Fig. 8. Logarithm (log_{10}) of molar concentration of (a) major and (b) minor components as a function of pH for the Sr(II) recovery for the expected brine (scenario 4). Points: experimental data, lines: PHREEQC simulation.

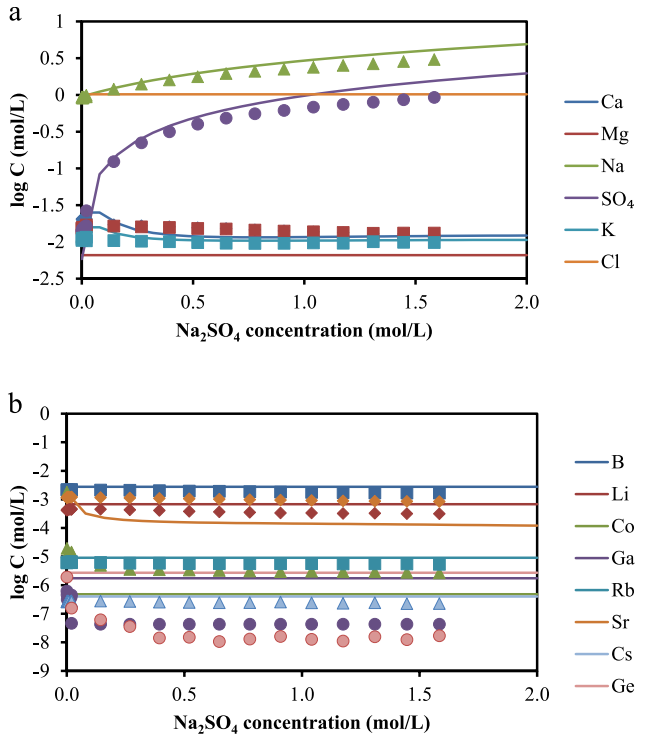

Fig. 9. Logarithm (log_{10}) of molar concentration of (a) major and (b) minor components as a function of Na_2SO_4(s) concentration added for the Sr(II) recovery for the expected brine (scenario 4) after reaching pH 10. Points: experimental data, lines: PHREEQC simulation.

mineral phases as $CoCO_3$(s) could be postulated as recovery route. In this way, despite they used a solution containing 800 mg/L Co and Cu, Quiton et al. [47] reported that higher Co removal could be achieved at pH 10 by using Na_2CO_3(s) as a precipitant rather than the one reached using NaOH(s). In Fig. S13 (Supplementary information) the solubility diagrams of Co(II) with hydroxides and carbonates is compared. The stability of $CoCO_3$(s) is much higher than $Co(OH)_2$(s) at neutral pH conditions allowing the precipitation of $CoCO_3$(s) and avoiding the co-precipitation of Mg(II).

The collected solids at pH 5 and 10 were analysed by FESEM-EDS (Fig. S14). The EDS spectra shows that crystals at pH 5 (Fig. S14.a) were made mainly of Ga and O, indicating the potential presence of mineral phases as GaOOH(s), and Na and Cl, probably NaCl(s) from morphology of the particles. Additionally, traces of Co(II) were observed in the collected solids. Fig. S14.b shows the FESEM images of the collected precipitates at pH 10. From EDS spectra (Fig. S14.b), it can be observed that solids are rich in Na and Cl, as NaCl probably, with a high presence of solids rich in Mg and O, mainly $Mg(OH)_2$(s) according to the morphology of the crystals. Additionally, Co was detected within the particles, probably present as $Co(OH)_2$(s), although at very low contents. As seen in the previous case, PHREEQC was able to predict the predominant presence of $Mg(OH)_2$(s) and also the precipitation of Co(II) and Ga(III) (see Supplementary Information, Fig. S15).

Finally, Sr(II) recovery (scenario 4) was studied. In this case, NaOH was first added from pH 0 to 10 and solids were collected at pH 5 and 10 to recover Ga(III) and Co(II), respectively (Fig. 8) and then, Na_2SO_4(s) was added to the solution (Fig. 9) in order to promote the precipitation of celestite ($SrSO_4$(s)).

Experimental results show that part of the Co(II) precipitated as $Co(OH)_2$(s) at pH 10, representing a recovery of 9 ± 1 %, whereas 77 ± 3 % of Ga(III) was recovered as GaOOH(s) at pH 5. Taking into account the PHREEQC predictions, it is expected the complete precipitation of Co(II) starting at pH 8 and that >95 % Ga(III) precipitate at pH 5. As in the previous case, the precipitation of $Mg(OH)_2$(s) is expected at pH higher than 9.5.

After Ga(III) and Co(II) reactive precipitation using 1 M NaOH, Na_2SO_4(s) was added. As shown in Fig. 9, PHREEQC simulation describes that, as soon as Na_2SO_4(s) was added to the solution, $SrSO_4$(s) should begin to precipitate, being the solution completely depleted on it after adding 0.5 mol/L (>95 % recovery). However, even reaching a 1.5 M concentration, its precipitation was slightly observed. In fact, considering both stages of the process (pH increase with NaOH and Na_2SO_4(s) addition), just a 55 % of the initial Sr(II) could be recovered.

It can also be observed that, adding Na_2SO_4(s), some Co(II), Ga(III) and Ge(IV) precipitation occurred, which may be related to a reaction where $CoSO_4$, $Ga_2(SO_4)_3$ and $Ge(SO_4)_2$ were formed. It must be noticed that, before adding Na_2SO_4(s), two filtration steps were performed after increasing the pH to 5 and 10 with NaOH to recover Ga(III) and Co(II), respectively, as hydroxides. Therefore, taking into account both steps (NaOH-filtration and Na_2SO_4(s) additions), >99 % of Co(II), Ga(III) and Ge(IV) were recovered. That could be related to the fact that the previous precipitated solids could sorb those elements.

Comparing these results to the ones obtained for scenario 3, Ga(III) would have been recovered mainly as GaOOH(s) due to NaOH, since >99 % was recovered in both scenarios and Na_2SO_4(s) was not used in scenario 3.

Fig. S16 shows images of the collected precipitates at pH 10. From EDS spectra, it can be observed that crystals were made of Na and Cl, as NaCl(s), Co and O, probably $Co(OH)_2$(s), and Mg and O, presumably Mg $(OH)_2$(s). This could be confirmed by PHREEQC prediction (see Supplementary Information, Fig. S17). Besides, traces of other elements (K, Ga) were present in the sample.

From the experiments performed from solutions mimicking a separation scheme where the partial selectivity of the sorbents are providing medium to selective separation (scenarios 1–4) the highest recovery factors (%) that could be achieved are summarized in Table 4. Values obtained for multi-component solutions were comparable with those from single-component solutions (Table 3).

Considering that experimental conditions for the recovery of different TEs were similar, a flowchart is provided in Fig. 10 to illustrate

Table 4
Maximum recovery factor (%) for the target TEs from the concentrated streams generated in the ion exchange (sorption extraction stage, scenarios 1–4), the reagent and energy (thermal/electrical) for mineral phase formation and the mineral composition of the recovered by-products. Initial concentration of the target TEs and the conditions under which the solids were obtained are provided.

Element	Initial concentration (mg/L)	Route for recovery	Reagent or energy	By-product mineral composition	Recovery (%)	Conditions
B(III)	1841 (scenario 1) 1235 (scenario 2)	Evaporation	Heat electrical energy	H_3BO_3(s)	76 % (scenario 1) 24 % (scenario 2)	90 % water evaporated
Ga(III)	45 (scenario 3) 0.12 (scenario 4)	Reactive precipitation	1.0 M NaOH	GaOOH(s)	>99 % (scenario 3) >99 % (scenario 4)	pH 5 (scenario 3) 1.58 mol/L of Na_2SO_4 (scenario 4)
Co(II)	56 (scenario 3) 135 (scenario 4)	Reactive precipitation	1.0 M NaOH	$Co(OH)_2$(s)	7 % (scenario 3) >99 % (scenario 4)	pH 10 (scenario 3) 1.58 mol/L of Na_2SO_4 (scenario 4)
Ge(IV)	0.09 (scenario 3) 0.20 (scenario 4)	Reactive precipitation	1.0 M NaOH	GeO_2(s)	17 % (scenario 3) >99 % (scenario 4)	pH 10 (scenario 3) 1.58 mol/L of Na_2SO_4 (scenario 4)
Sr(II)	152 (scenario 4)	Reactive precipitation	Na_2SO_4(s)	$SrSO_4$(s)	55 % (scenario 4)	1.58 mol/L of Na_2SO_4

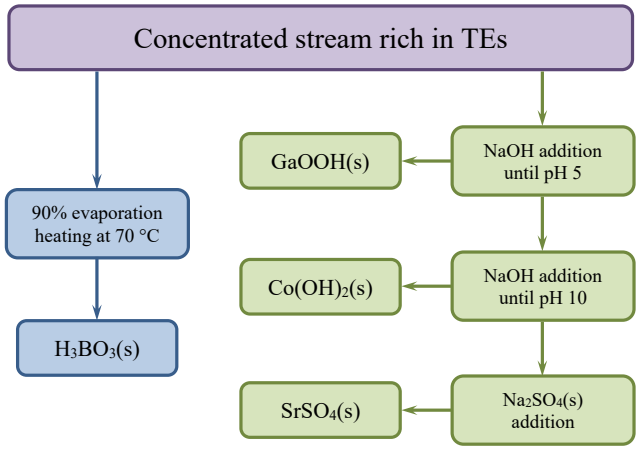

Fig. 10. Potential sequential metal recovery scheme.

the different routes to precipitate and recover the TEs of interest.

Based on the speciation diagrams (Fig. 3, Figs. S1–S4) and the FESEM-EDS and XRD analysis of the solids obtained (Figs. S5–S10, Fig. S12, Fig. S14 and Fig. S16), Table 5 collects some of the EDS spectrum of the solids obtained in the performances of multi-component solutions and the mineral phase that was expected to be obtained. These results showed that, despite having some difficulties to obtain H_3BO_3(s) and $Co(OH)_2$(s) in scenarios 2 and 3, respectively, the routes suggested and followed within this study to crystallise the targeted TEs are potentially viable.

4. Conclusions

Single-component solutions experiments simulating scenarios of applying sorbents with high selectivity factors showed that Co(II) and Ga(III) could be completely recovered as hydroxides (β-$Co(OH)_2$(s) and GaOOH(s)) by precipitation with NaOH. In the evaluated range (200 mg/L) recoveries of >99 % were achieved for both Co(II) and Ga(III). In the case of Sr(II), it is more efficient to precipitate it as celestite ($SrSO_4$(s)) by adding Na_2SO_4(s) due to the high solubility of $Sr(OH)_2$(s). Similarly, B(III) compounds solubility made precipitation unlikely, so an evaporative route was explored, achieving an effective recovery of 51 %. However, Ge(IV) was not recovered by NaOH precipitation even if its concentration was increased up to 1 g/L. Ge(IV) recovery, as GeO_2(s), using chemicals generated from saltworks bitterns is not feasible, as it is requested to use tannic acid or sulphide/hydrogen sulphide solutions, as several studies pointed out as an alternative route to precipitate it.

Regarding the multi-component solutions experiments carried out (assuming the use of sorbent with limited TEs selectivities), high content of NaCl precipitated in all the cases when crystallisation was applied. This is due to HCl content in the solutions since they mimic the outcome of an elution process of ion exchange columns. Therefore, the acid should be removed before crystallisation recovery. Moreover, the necessity of a concentration step was noted before the crystallisation under the assumed scenarios, since the results showed that the actual composition was not enough to achieve the saturation level of the mineral phases.

PHREEQC was able to predict the experimental trends obtained in most cases for both single- and multi-component solutions. Discrepancies between experimental data and PHREEQC predictions were only found for Sr(II) and Ga(III), where the precipitation was predicted at lower pH values.

Table 5
Semi-quantitative analysis (% weight) given by the EDS spectra of the collected precipitates from each multi-component solution (scenarios 1–4).

Scenario	EDS spectrum												Expected solid
	B	O	Na	Mg	Al	Si	S	Cl	K	Ca	Co	Ga	
1	23.5	76.5	-	-	-	-	-	-	-	-	-	-	H_3BO_3(s)
2	1.4	71.5	11.1	-	0.5	-	0.4	14.7	-	0.4	-	-	H_3BO_3(s)
3[a]	-	10.7	17.3	-	-	-	1.9	35.3	-	-	-	34.9	GaOOH(s)
3[b]	-	3.2	37.3	3.4	-	-	-	55.5	-	-	0.7	-	$Co(OH)_2$(s)
4[b]	-	34.6	3.7	6.9	1.3	0.7	-	15.6	0.7	1.0	34.0	1.3	$Co(OH)_2$(s)

[a] Precipitates collected at pH 5.
[b] Precipitates collected at pH 10.

Declaration of Competing Interest

The authors declare that they have no known competing financial interests or personal relationships that could have appeared to influence the work reported in this paper.

Data availability

The data will be available in Zenodo.

Acknowledgements

This work was supported by the EU within SEArcularMINE (Circular Processing of Seawater Brines from Saltworks for Recovery of Valuable Raw Materials) project – Horizon 2020 programme, Grant Agreement No. 869467. This output reflects only the author's view. The European Health and Digital Executive Agency (HaDEA) and the European Commission cannot be held responsible for any use that may be made of the information contained therein. This study has been also supported by the Research Spanish Agency (AEI) through the Resources recycling from agri-food urban and industrial wastes by integration of hybrid separation processes (W4V) project (PID2020-114401RB-C21) and the Catalan Agaur Agency through the 2017SGR312. Additionally, the authors acknowledge the OpenInnovation – Research Translation and Applied Knowledge Exchange in Practice through University-Industry-Cooperation (OpenInnoTrain), Grant Agreement Number (GAN): 823971, H2020-MSCA-RISE-2018-823971.

Appendix A. Supplementary material

Supplementary data to this article can be found online at https://doi.org/10.1016/j.seppur.2022.122622.

References

[1] European Commission, Study on the EU's list of Critical Raw Materials - Critical Raw Materials Factsheets, 2020, doi: 10.2873/92480.
[2] R. Pell, L. Tijsseling, K. Goodenough, F. Wall, Q. Dehaine, A. Grant, D. Deak, X. Yan, P. Whattoff, Towards sustainable extraction of technology materials through integrated approaches, Nat. Rev. Earth Environ. 2 (2021) 665–679, https://doi.org/10.1038/s43017-021-00211-6.
[3] A.S. Bello, N. Zouari, D.A. Da'ana, J.N. Hahladakis, M.A. Al-Ghouti, An overview of brine management: emerging desalination technologies, life cycle assessment, and metal recovery methodologies, J. Environ. Manage. 288 (2021), doi: 10.1016/j.jenvman.2021.112358.
[4] R.S. Al-Absi, M. Abu-Dieyeh, M.A. Al-Ghouti, Brine management strategies, technologies, and recovery using adsorption processes, Environ. Technol. Innovation 22 (2021), 101541, https://doi.org/10.1016/j.eti.2021.101541.
[5] B.K. Pramanik, L.D. Nghiem, F.I. Hai, Extraction of strategically important elements from brines: constraints and opportunities, Water Res. 168 (2020), 115149, https://doi.org/10.1016/j.watres.2019.115149.
[6] A. Kumar, G. Naidu, H. Fukuda, F. Du, S. Vigneswaran, E. Drioli, J.H. Lienhard, Metals recovery from seawater desalination brines: technologies, opportunities, and challenges, ACS Sustain. Chem. Eng. 9 (23) (2021) 7704–7712.
[7] M.S. Diallo, M.R. Kotte, M. Cho, Mining critical metals and elements from seawater: opportunities and challenges, Environ. Sci. Technol. 49 (2015) 9390–9399, https://doi.org/10.1021/acs.est.5b00463.
[8] X. Zhang, W. Zhao, Y. Zhang, V. Jegatheesan, A review of resource recovery from seawater desalination brine, Rev. Environ. Sci. Biotechnol. 20 (2021) 333–361, https://doi.org/10.1007/s11157-021-09570-4.
[9] M. Reig, C. Valderrama, O. Gibert, J.L. Cortina, Selectrodialysis and bipolar membrane electrodialysis combination for industrial process brines treatment: monovalent-divalent ions separation and acid and base production, Desalination 399 (2016) 88–95, https://doi.org/10.1016/j.desal.2016.08.010.
[10] M. Reig, S. Casas, O. Gibert, C. Valderrama, J.L. Cortina, Integration of nanofiltration and bipolar electrodialysis for valorization of seawater desalination brines: production of drinking and waste water treatment chemicals, Desalination 382 (2016) 13–20, https://doi.org/10.1016/j.desal.2015.12.013.
[11] M. Reig, S. Casas, C. Valderrama, O. Gibert, J.L. Cortina, Integration of monopolar and bipolar electrodialysis for valorization of seawater reverse osmosis desalination brines: production of strong acid and base, Desalination 398 (2016) 87–97, https://doi.org/10.1016/j.desal.2016.07.024.
[12] J. Yang, X. Luo, T. Yan, X. Lin, Recovery of cesium from saline lake brine with potassium cobalt hexacyanoferrate-modified chrome-tanned leather scrap adsorbent, Colloids Surf., A 537 (2018) 268–280, https://doi.org/10.1016/j.colsurfa.2017.10.015.
[13] O. Gibert, C. Valderrama, M. Peterkóva, J.L. Cortina, Evaluation of selective sorbents for the extraction of valuable metal ions (Cs, Rb, Li, U) from reverse osmosis rejected brine, Solvent Extract. Ion Exchange 28 (2010) 543–562, https://doi.org/10.1080/07366299.2010.480931.
[14] S.M. Liu, H.H. Liu, Y.J. Huang, W.J. Yang, Solvent extraction of rubidium and cesium from salt lake brine with t-BAMBP-kerosene solution, Trans. Nonferrous Met. Soc. China (Engl. Ed.) 25 (2015) 329–334, https://doi.org/10.1016/S1003-6326(15)63608-1.
[15] G. Naidu, S. Jeong, Y. Choi, M.H. Song, U. Oyunchuluun, S. Vigneswaran, Valuable rubidium extraction from potassium reduced seawater brine, J. Cleaner Prod. 174 (2018) 1079–1088, https://doi.org/10.1016/j.jclepro.2017.11.042.
[16] G. Naidu, S. Jeong, M.A.H. Johir, A.G. Fane, J. Kandasamy, S. Vigneswaran, Rubidium extraction from seawater brine by an integrated membrane distillation-selective sorption system, Water Res. 123 (2017) 321–331, https://doi.org/10.1016/j.watres.2017.06.078.
[17] D. Alby, C. Charnay, M. Heran, B. Prelot, J. Zajac, Recent developments in nanostructured inorganic materials for sorption of cesium and strontium: synthesis and shaping, sorption capacity, mechanisms, and selectivity—a review, J. Hazard. Mater. 344 (2018) 511–530, https://doi.org/10.1016/j.jhazmat.2017.10.047.
[18] Y. Takahatake, A. Shibata, K. Nomura, T. Sato, Effect of flowing water on Sr sorption changes, Minerals 7 (2017), https://doi.org/10.3390/min7120247.
[19] N. Ghaeni, M.S. Taleshi, F. Elmi, Removal and recovery of strontium (Sr(II))from seawater by Fe3O4/MnO2/fulvic acid nanocomposite, Mar. Chem. 213 (2019) 33–39, https://doi.org/10.1016/j.marchem.2019.05.003.
[20] G. Wang, Y. Zhang, S. Jiang, X. Ma, B. Wei, Removal and recovery of cobalt from Co(II)–containing water samples by dithiocarboxyl polyethyleneimine, Sep. Purif. Technol. 251 (2020) 1–9, https://doi.org/10.1016/j.seppur.2020.117338.
[21] F. Lu, T. Xiao, J. Lin, Z. Ning, Q. Long, L. Xiao, F. Huang, W. Wang, Q. Xiao, X. Lan, H. Chen, Resources and extraction of gallium: a review, Hydrometallurgy 174 (2017) 105–115, https://doi.org/10.1016/j.hydromet.2017.10.010.
[22] V.N. Sagdiev, O.V. Cheremisina, M.A. Ponomareva, E.S. Zatula, Process of extraction of gallium from technological solutions with the use of ion exchange resins, Metallurgist 63 (2019) 206–214, https://doi.org/10.1007/s11015-019-00811-0.
[23] Z. Zhao, Y. Yang, Y. Xiao, Y. Fan, Recovery of gallium from Bayer liquor: a review, Hydrometallurgy 125–126 (2012) 115–124, https://doi.org/10.1016/j.hydromet.2012.06.002.
[24] S. Virolainen, E. Paatero, Ion exchange recovery of germanium from sulfate solutions with N-methylglucamine functional resin, in: By-Product Metals in Non-Ferrous Metals Industry, 2013, https://www.researchgate.net/publication/281430287.
[25] S. Nusen, Z. Zhu, T. Chairuangsri, C.Y. Cheng, Recovery of germanium from synthetic leach solution of zinc refinery residues by synergistic solvent extraction using LIX 63 and Ionquest 801, Hydrometallurgy 151 (2015) 122–132, https://doi.org/10.1016/j.hydromet.2014.11.016.
[26] N. Taylan, H. Gürbüz, A.N. Bulutcu, Effects of ultrasound on the reaction step of boric acid production process from colemanite, Ultrason. Sonochem. 14 (2007) 633–638, https://doi.org/10.1016/j.ultsonch.2006.11.001.
[27] M.M. Nasef, M. Nallappan, Z. Ujang, Polymer-based chelating adsorbents for the selective removal of boron from water and wastewater: a review, React. Funct. Polym. 85 (2014) 54–68, https://doi.org/10.1016/j.reactfunctpolym.2014.10.007.
[28] M. Tagliabue, A.P. Reverberi, R. Bagatin, Boron removal from water: needs, challenges and perspectives, J. Cleaner Prod. 77 (2014) 56–64, https://doi.org/10.1016/j.jclepro.2013.11.040.
[29] W. Xiang, S. Liang, Z. Zhou, W. Qin, W. Fei, Extraction of lithium from salt lake brine containing borate anion and high concentration of magnesium, Hydrometallurgy 166 (2016) 9–15, https://doi.org/10.1016/j.hydromet.2016.08.005.
[30] L. Bonin, D. Deduytsche, M. Wolthers, V. Flexer, K. Rabaey, Boron extraction using selective ion exchange resins enables effective magnesium recovery from lithium rich brines with minimal lithium loss, Sep. Purif. Technol. 275 (2021), https://doi.org/10.1016/j.seppur.2021.119177.
[31] V. Vallès, J. López, M. Fernández de Labastida, O. Gibert, A. Leskinen, R. T. Koivula, J.L. Cortina, Polymeric and inorganic sorbents for a green option to recover critical raw materials at trace levels from sea saltworks bitterns, Green Chem. (2022). Under Review.
[32] SEArcularMINE, Circular Processing of Seawater Brines from Saltworks for Recovery of Valuable Raw Materials - SEArcularMINE, 2020, https://searcularmine.eu/ (accessed May 9, 2021).
[33] W.M. Haynes, D.R. Lide, T.J. Bruno, CRC Handbook of Chemistry and Physics, 94th ed., CRC Press, Boca Raton, 2013.
[34] Kirk-Othmer, Encyclopedia of Chemical Technology, 4th ed., John Wiley and Sons, New York, 1992.
[35] R.D. Ashford, Ashford's Dictionary of Industrial Chemicals, Wavelength Publications Ltd., London, England, 1994.
[36] C.H. Bingham, E. Cohrssen, B. Powell, Patty's Toxicology, 5th ed., John Wiley & Sons, New York, 2001.
[37] International Labour Organization, ILO-WHO International Chemical Safety Cards (ICSC), 2021.
[38] National Institute for Occupational Safety and Health/Occupational Safety and Health Administration, Occupational Health Guidelines for Chemical Hazards, DHHS/NIOSH, Government Printing Office, Cincinnati, U.S., 1981.
[39] F. Vicari, S. Randazzo, J. López, M.F. de Labastida, V. Vallès, G. Micale, A. Tamburini, G.D. Staiti, J.L. Cortina, A. Cipollina, M. Fernández de Labastida,

V. Vallès, G. Micale, A. Tamburini, G. D'Alì Staiti, J.L. Cortina, A. Cipollina, Mining minerals and critical raw materials from bittern: understanding metal ions fate in saltwork ponds, Sci. Total Environ. 847 (2022), https://doi.org/10.1016/j.scitotenv.2022.157544.

[40] D.L. Parkhurst, C.A.J. Appelo, Description of input and examples for PHREEQC version 3—a computer program for speciation, batch-reaction, one-dimensional transport, and inverse geochemical calculations, in: U.S. Geological Survey Techniques and Methods, Book 6, Chap. A43, 497p., Denver, Colorado, 2013.

[41] M. Drzazga, A. Chmielarz, G. Benke, K. Leszczyńska-Sejda, M. Knapik, P. Kowalik, M. Ciszewski, Precipitation of germanium from sulphate solutions containing tin and indium using tannic acid, Appl. Sci. (Switzerland) 9 (2019), https://doi.org/10.3390/app9050966.

[42] F. Arroyo Torralvo, C. Fernández-Pereira, E. García Villard, Y. Luna, C. Leiva, L. Vilches, R. Villegas, Low environmental impact process for germanium recovery from an industrial residue, Miner. Eng. 128 (2018) 106–114, https://doi.org/10.1016/j.mineng.2018.07.022.

[43] S. Bayat, S. Aghazadeh, M. Noaparast, M. Gharabaghi, B. Taheri, Germanium separation and purification by leaching and precipitation, J. Cent. South Univ. 23 (2016) 2214–2222, https://doi.org/10.1007/s11771-016-3279-6.

[44] D. Liang, J. Wang, Y. Wang, F. Wang, J. Jiang, Behavior of tannins in germanium recovery by tannin process, Hydrometallurgy 93 (2008) 140–142, https://doi.org/10.1016/j.hydromet.2008.03.006.

[45] F. Arroyo, O. Font, C. Fernández-Pereira, X. Querol, R. Juan, C. Ruiz, P. Coca, Germanium recovery from gasification fly ash: evaluation of end-products obtained by precipitation methods, J. Hazard. Mater. 167 (2009) 582–588, https://doi.org/10.1016/j.jhazmat.2009.01.021.

[46] A.E. Yilmaz, R. Boncukcuoğlu, S. Bayar, B.A. Fil, M.M. Kocakerim, Boron removal by means of chemical precipitation with calcium hydroxide and calcium borate formation, Korean J. Chem. Eng. 29 (2012) 1382–1387, https://doi.org/10.1007/s11814-012-0040-1.

[47] K.G.N. Quiton, Y.-H. Huang, M.-C. Lu, Recovery of cobalt and copper from single- and co-contaminated simulated electroplating wastewater via carbonate and hydroxide precipitation, Sustain. Environ. Res. 32 (2022), https://doi.org/10.1186/s42834-022-00140-z.